

Determination of Lüders Strains and Flow Properties in Steels from Hardness / Microhardness Tests

FAHMY M. HAGGAG and GLENN E. LUCAS

Development of radiation tolerant materials for use in fusion reactors requires testing of small volumes of candidate materials in high energy neutron irradiation facilities. As part of an effort to develop methods for extracting mechanical property information from small specimens, this study investigated techniques to characterize flow properties of steels exhibiting Lüders strains from ball indentation hardness/microhardness tests. A quantitative relationship was found between the amount of pile-up formed during indentation and the magnitude of the Lüders strain exhibited during tensile testing in SAE 1015 steel. Moreover, by nonlinear regression analysis, a single set of equations was found which correlated hardness data to the homogeneous true-stress-true-plastic strain relationship of steels in a variety of metallurgical conditions in the strain range of 1 to 10 pct at room temperature.

I. INTRODUCTION

THE development of structural alloys suitable for use in fusion reactors is an international effort, and it is currently one of the great challenges in metallurgy. For instance, anticipated lifetime levels of atomic displacement effected by the bombardment of first-wall materials by high energy (14 MeV) neutrons are nominally 100 displacements per atom (dpa). The dimensional changes and mechanical property degradation this damage produces can be most dramatic; moreover, such damage may be severely aggravated by the buildup of transmutants, particularly helium, which may be produced at rates of 5 to 30 appm He/dpa.¹ The development of alloys to withstand this punishment cannot proceed by empiricism alone, but requires a fundamental understanding of the effects of high energy neutron irradiation on the microstructure and mechanical properties of candidate materials.

To this end, the test environments of both fission reactors and high energy neutron sources, such as the Rotating Target Neutron Source (RTNS-II),² will be used over the near term to obtain the necessary data to develop this understanding. However, because of the large number of materials under consideration and the volume constraints in these test environments, a key element in the program is the development of test techniques to extract mechanical property information from specimens which are small in size and have perhaps a multipurpose geometry. Transmission electron microscopy (TEM) discs are an example.

To date a number of efforts in small specimen testing have been initiated.^{3,4,5,6,7,8,9,10,11,12} One of these, instrumented hardness/microhardness,³ has been used successfully to correlate hardness data obtained with a spherical indenter with points on the true-stress-true-plastic strain curve over a strain range of 0.7 pct to 10 pct. This has been achieved for a variety of materials. However, in the initial studies the instrumented hardness data did not correlate well with true-stress-strain curves for steels exhibiting Lüders strain.³

Yet there is interest in applying the instrumented hardness/microhardness test to steels exhibiting Lüders strain. High chromium tempered martensitic steels are one class of alloys under consideration for fusion reactors. Moreover, the instrumented hardness test may have more general application than the fusion reactor materials development program, e.g., in the examination of both nuclear and nonnuclear applications. Consequently, this study was undertaken to (1) determine a methodology for predicting flow properties in steels exhibiting Lüders strain from hardness/microhardness data and (2) develop a technique for predicting the magnitude of Lüders strains in steels from the characterization of the geometry of a spherical indentation.

II. MATERIALS CHARACTERIZATION

The base material used in this study was SAE No. 1015 steel supplied by Ducommun Metals as cold rolled sheet, 0.124 cm thick. Tensile specimens were fabricated from as-received sheet stock, and sets of tensile specimens were aged at different temperatures for 20 minutes; the aging temperatures ranged from 121 to 621°C. A total of 47 specimens was heat treated. These specimens were then pulled in tension by means described shortly, and the value of Lüders strain was obtained directly from the load-displacement data. The values of Lüders strains exhibited as a function of aging temperature are shown in Figure 1, where the line represents a polynomial fit to the data. The Lüders strain, which ranged from 0.48 pct to 6.0 pct, initially increased with aging temperature and then decreased, in agreement with previous observations by other investigators.^{13,14}

Based on these results, nine representative samples were selected for further hardness and microhardness examination. These are listed in Table I. The average grain diameter for all these nine specimens was 20 μm . The tensile data of the nine selected specimens were fit by linear regression analysis to a relation between a true-stress, σ_t , and true-plastic-strain, ϵ_p , which was assumed to be of the form:

$$\begin{aligned}\sigma_t &= \sigma_{ly} \text{ for } \epsilon_p < \epsilon_L \\ \sigma_t &= K\epsilon_p^n \text{ for } \epsilon_p \geq \epsilon_L\end{aligned}\quad [1]$$

FAHMY M. HAGGAG, Senior Engineer, is with Nuclear Safety Methods Division, EG&G Idaho, Inc., PO Box 1625, Idaho Falls, ID 83415. GLENN E. LUCAS, Associate Professor, is with the Department of Chemical and Nuclear Engineering, University of California, Santa Barbara, CA 93106.

Manuscript submitted December 13, 1982.

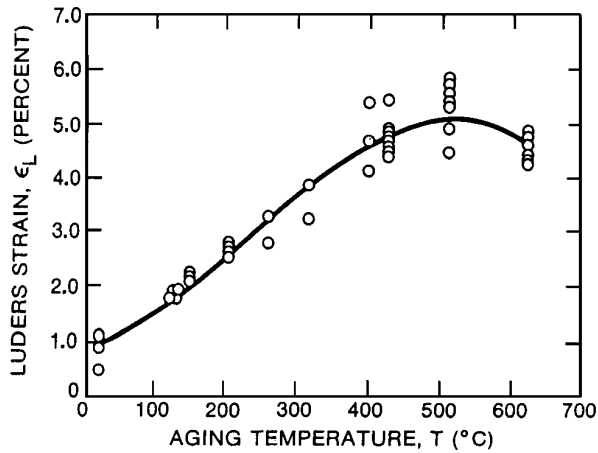


Fig. 1 – The dependence of Lüders strain on aging temperature.

**Table I. Regression Parameters
Obtained from Tensile Test Data**

Specimen Designation	ϵ_L (Pct)	σ_{ly} (MPa)	K (MPa)	n
S2	0.88	245	473	0.14
S4	1.74	257	478	0.15
S6	2.16	272	495	0.15
S8	2.76	281	484	0.15
S10	3.25	290	533	0.18
S11	3.86	293	534	0.18
S15	4.70	301	597	0.22
S18	4.80	281	615	0.26
S20	5.40	296	605	0.24

where σ_{ly} is the lower yield stress, K is a constant, and n is the strain-hardening exponent. Values of these parameters are also given in Table I. The lower yield stress increased with aging temperature and then decreased; this is consistent with the aging temperature dependence of Lüders strain^{13, 14} as previously noted. The regression parameters, n and K , increased with Lüders strain; and $\log \sigma_{ly}$ was found to increase linearly with $\log \epsilon_L$, in agreement with the results of Tanaka and Ishikawa.¹⁵ The regression equations are shown in normalized, composite form in Figure 2 to illustrate the basic differences in Lüders strain and work-hardening behavior among the materials.

III. EXPERIMENTAL PROCEDURE

Tensile specimens were machined from 1015 steel sheet, with their axes aligned with the longitudinal direction of the sheet. The uniaxial tension tests were performed at room temperature on an Instron 1122 mechanical testing machine in conformance with ASTM Standard E8-76, with the exception of a modified sample geometry which is shown in Figure 3. All tests were performed with a cross-head speed of 0.002 cm/s (0.05 in/min). Specimen gage length deformation was monitored by a standard clip gage with a resolution of 1.27×10^{-4} cm (5×10^{-5} in). All load-displacement data were converted to true-stress, true-plastic-strain data for values of strain less than the uniform strain.

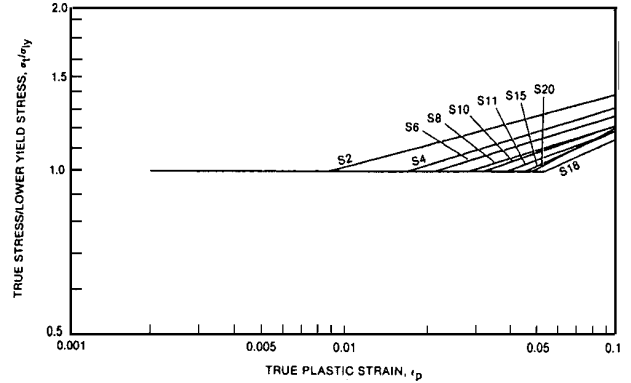


Fig. 2 – Log-log plot of normalized true stress vs true plastic strain for 9 selected steel specimens.

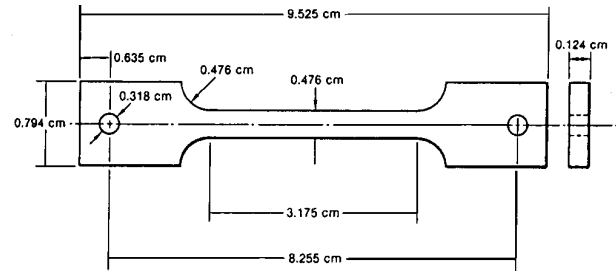


Fig. 3 – Tensile test specimen geometry.

The hardness/microhardness specimens consisted of 0.79 cm x 1.3 cm coupons obtained from the undeformed end tabs of the tensile specimens after they were tested. Tests performed with a mechanical testing machine are referred to here as “hardness” tests, while those performed with the microhardness tester are referred to here as microhardness tests.

Hardness tests were performed with a Rockwell-type ball indenter of 0.159 cm diameter. The ball indenter was attached to the load cell of an Instron 1122 testing machine. The specimens were positioned on a fixed platen stage below the cross-head; and the latter was driven at a constant speed of 8.5×10^{-5} cm/s (0.002 in/min), which in turn drove the indenter into the specimen. When the desired load was obtained the cross-head direction was reversed. Each specimen was indented several times at different locations with loads ranging from 0.90 kg to 18.15 kg. Each indentation diameter was then determined optically with a filar microscope attached to a Wilson Tukon® microhardness tester.

The microhardness tests were also performed at room temperature on the same Wilson Tukon® microhardness tester, which was modified to use a 0.0254 cm diameter steel ball as an indenter. Two multiple indentations were made in each specimen. These indentations were obtained by incrementally increasing the load from 200 grams to 1100 grams. The multiple indentation technique was justified by a set of scooping experiments in which the diameter of an indentation made by multiple loadings to some maximum load was compared to that made by a single loading to the same maximum load; no differences were found. The effective initial indenter speed for the Wilson Tukon® microhardness tester was 0.1 cm/min (0.04 in/min), and loads were automatically applied for approximately 20 seconds. Following each indentation, the indentation diameter

was measured optically with the filar microscope supplied with the Tukon®.

The geometries of the indentations were characterized by two methods, namely, profilometer measurements and optical interference measurements. The profilometer measurements were made with a Bendix RCC-4 profilometer. The profiles or indentations made with a load of 18.15 kg (40 pounds) on each of the hardness specimens were analyzed. A typical profilometer trace is shown in Figure 4. A number of geometric features of the indentation were taken directly from the profiles. These were the indentation chordal diameter, d , maximum lip height, h_l , and the width of the lip at half its maximum height, $w_{1/2}$. In addition, the area of the lip, A , surrounding the indentation, as defined by the hatched area in Figure 4, was measured using a planimeter. Profilometer traces of the indentations were obtained and analyzed for traces taken in both the longitudinal and transverse directions of the sheet material, and average values of lip geometry features were determined.

There were several difficulties with this technique. Because of the small size of the indentations, centerline traces were difficult to achieve, and hence the process was somewhat tedious and time consuming. The stylus also left a permanent scratch through the indentation. In addition, the indentations deviated from axisymmetry (that is, h_l , $w_{1/2}$, and area under the lip on one side of the indentation was frequently quite different from values on the other side). And this was not easily mapped around the lip circumference with profilometry. Consequently, optical interference techniques were briefly investigated as an alternative method of characterizing indentation geometries. Indentations made at 9.07 kg (20 pounds) were examined on a Unitron® Series N metallograph. This load was chosen to provide an indentation of optimum size for photographic recording, given the magnification limitations of the interference system. Optical interferometry was performed with a xenon light source using a highly monochromatic cadmium filter; the wave length of the transmitted light was $\lambda = 644$ nm. Optical interferographs were obtained for indentations made in specimens having different values of Lüders strain.

IV. RESULTS

Uniaxial tensile Lüders strains were correlated with the ball indentation lip geometries obtained from profilometer measurements and optical measurements. In addition, the hardness/microhardness data were correlated with the corresponding uniaxial tension data. The results of these analyses are described in the following sections.

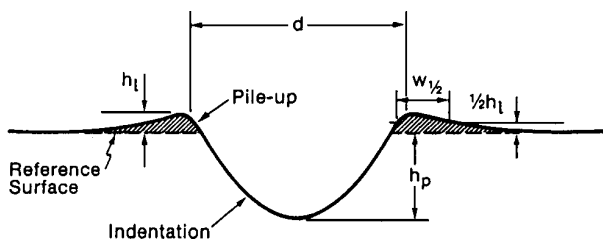


Fig. 4 – A typical profilometer trace of 1015 steel loaded at 9.07 kg (20 lbs).

A. Correlation between Lüders Strain and Lip Geometry

1. Profilometer Technique

The best quantitative correlation between lip geometry and Lüders strain was found for A , the area under the lip. A plot of the directional averaged value of A as a function of Lüders strain is shown in Figure 5. A linear regression of the data shows that

$$A = 4.24 \times 10^{-6} + 5.39 \times 10^{-5} \epsilon_L \text{ cm}^2 \quad [2]$$

where ϵ_L is the Lüders strain. It is worth noting here that the area of the lip for all the indents was measured at an areal magnification of 1.25×10^6 which obtained by planimetric analysis of a profilometer tracing with a magnification of 500 times for the X-axis (horizontal) and 2500 times for the Y-axis (vertical). The error bands in Figure 5 reflect the scatter in the value of A obtained by planimetric analysis of the lip on each side of the indentation for both transverse and longitudinal traces. The scatter is considerable in some cases, and the main reason discovered for this will be discussed shortly.

2. Optical Interference Technique

Three optical interferographs representative of the range of indentation geometries observed are presented in Figures 6. The horizontal axis of these photos corresponds to the rolling direction of the sheet material along which the superimposed profilometer traces were obtained. Each interference fringe corresponds to a 322 nm (half of the wavelength of the transmitted light, $\lambda/2$) displacement out of the plane of the paper. For increasing Lüders strain exhibited by the material, the number of interference fringes around the corresponding indentation increases. The increased number of interference fringes means an increase of the volume of material displaced (piled up) around these indentations and hence an increase in the overall plastic deformation. This is in agreement qualitatively with the trend illustrated previously in Figure 5. Thus, the interferographs provide an immediate and graphic correlation between the indentation geometry and the magnitude of the Lüders strain exhibited by the material.

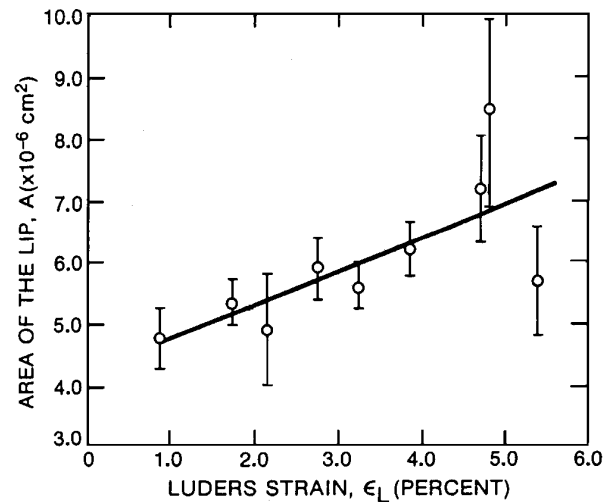


Fig. 5 – Relation between the area of the lip and Lüders strain for indentations obtained at 18.15 kg load with a ball indenter of 0.1588 cm diameter.

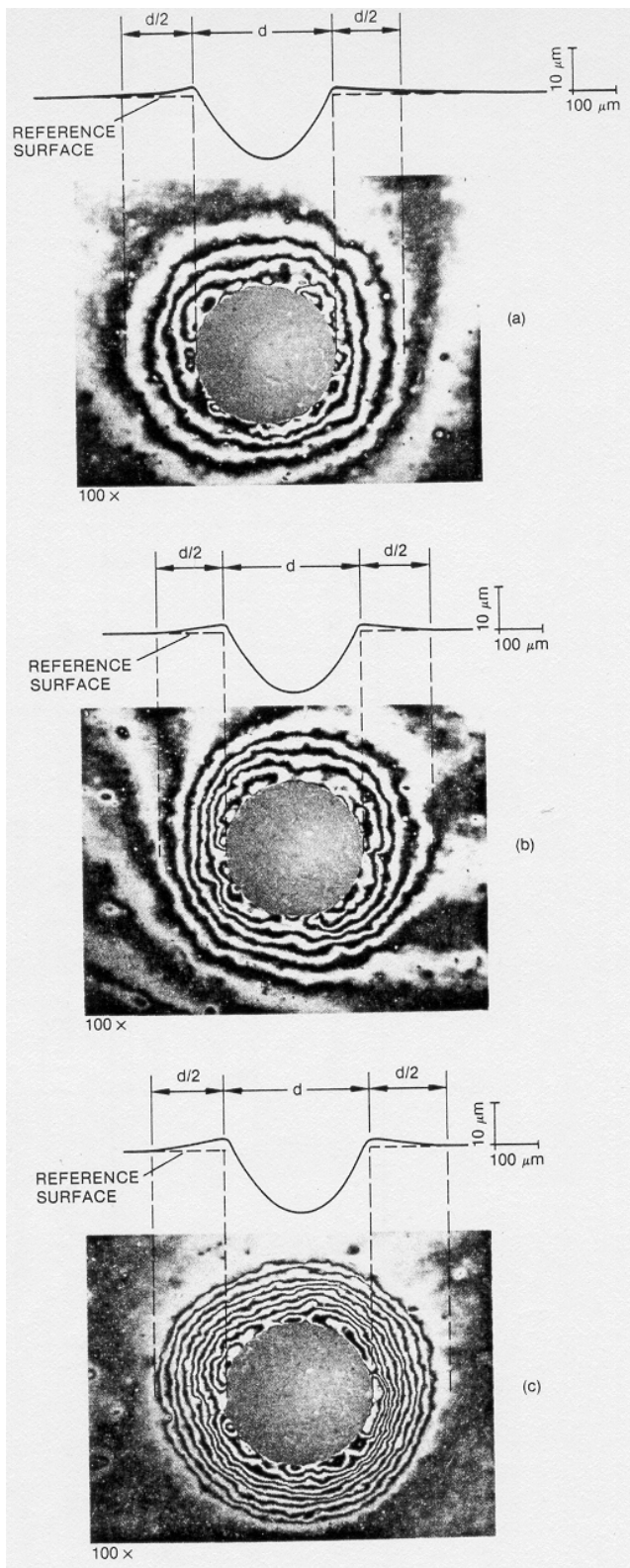


Fig. 6 – Profilometer traces and interferographs of indentation of 1015 steels made at 9.07 kg (20 lb): (a) S2 – as-received $-\epsilon_L = 0.88$ pct, (b) S8 – aged 20 min at 204 °C - $\epsilon_L = 2.76$ pct, and (c) S20 – aged 20 min at 621°C- $\epsilon_L = 4.8$ pct.

Quantitatively, the geometry of the indentations as characterized by both interferometry and profilometry techniques are also in good agreement. Values of the lip geometry features such as the indentation diameter, d , and the maximum lip height, h_l , as measured by both profilometric and optical techniques, were equivalent. Results for the three indentations given in Figure 6 are compared in Table II.

Another characteristic of the indentation geometry which became obvious during interferography is shown in Figure 6. That is, the lip of the indentation exhibits a set of nested fringes. This indicates the lip of the pile-up is crown-like in appearance. For a variety of materials examined, Underwood¹⁶ reported that this appeared only in steels, and he attributed this to the inhomogeneous plastic flow associated with Lüders band formation. This crowning behavior is one of the prime reasons for the asymmetry observed in the lip profiles obtained with profilometer. Hence, a complete three-dimensional characterization of the indentation is probably essential for an accurate correlation with flow properties like Lüders strain.

B. Correlation between Hardness/Microhardness Data and Tensile Data

Nonlinear regression analysis was used to obtain a set of equations to predict the homogeneous plastic flow part of the true-stress σ_t , true-plastic-strain, ϵ_p curve. The form of the equations was that used by Au *et al.*,³ who derived their correlation from the work of Tabor¹⁷ and Francis.¹⁸ The best fit was found for the following equations:

$$\epsilon_p = 0.2 d / D \quad [3]$$

$$\sigma_t = P_m / \psi = 4W / \pi d^2 \psi \quad [4]$$

where

$$\psi = \begin{cases} 1.07 & \phi \leq 1 \\ 1.07 + 0.759 \ln \phi & 1 < \phi < 24 \\ 3.48 & \phi \geq 24 \end{cases} \quad [5]$$

and

$$\phi = \epsilon_p E_2 / 0.43 \sigma_t \quad [6]$$

In the above equations, d is the chordal diameter of the indentation, D is the diameter of the ball indenter, P_m is the mean pressure between the surface of the indenter and the indentation, W is the applied load, and E_2 is the elastic modulus of the specimen.

Table II. Comparison of Chordal Diameters and Indentation Lip Heights Measured by Profilometric and Interferometric Techniques for the Indentations Given in Figure 6

Specimen Designation	$d(\mu\text{m})$		$h_l(\mu\text{m})$	
	Optical	Profilometer	Optical	Profilometer
S2	320 ± 3	326 ± 5	1.29 ± 0.16	1.4 ± 0.1
S8	318 ± 3	315 ± 5	1.45 ± 0.16	1.7 ± 0.1
S20	330 ± 3	340 ± 5	2.74 ± 0.16	2.7 ± 0.±

Comparison of the hardness-based $\sigma_t - \epsilon_p$ points with tensile data is provided for a representative range of samples in Figures 7 through 10. The circular points indicate hardness indentations made with a 1.59 mm diameter ball indenter using the Instron® mechanical testing machine, while the rectangular points represent microhardness indentations produced with a 0.25 mm diameter ball indenter, using the Tukon® microhardness tester. The uniaxial tensile data are represented by the solid curves, and the homogeneous flow portion of the curve is extrapolated to values of $\epsilon_p < \epsilon_L$ by the dotted line. As can be seen, the hardness data fit the homogeneous flow portion of the tensile curves well, over the whole range of samples investigated. Moreover, the correlation equations which provide this fit, Eqs. [3] through [5], have coefficients which are quite similar to those obtained previously for a wide range of materials.^{3,17,18} Reasons for differences are described below.

It should be noted that the microhardness data obtained at loads less than 200 grams were eliminated from the data set as outliers, since these data points had large residuals relative to the other data in the nonlinear regression analysis. Physically, this may be a result of the size of the indentation at these small loads, since indentations made at 200 g are comparable to the grain size, and smaller loads result in indentations which may intersect only one grain.

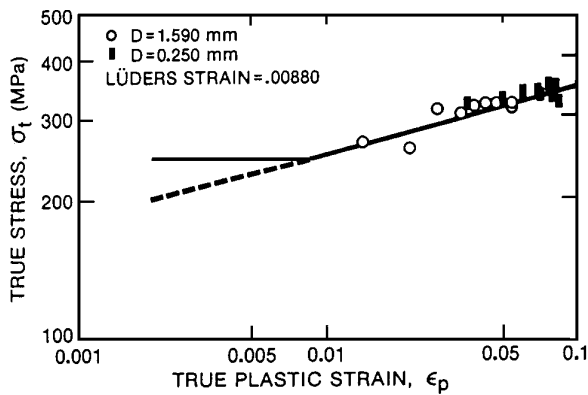


Fig. 7 – Comparison of the hardness/microhardness-derived stress-strain data to the uniaxial tensile stress-strain curve for 1015 steel in the as-received condition (S2).

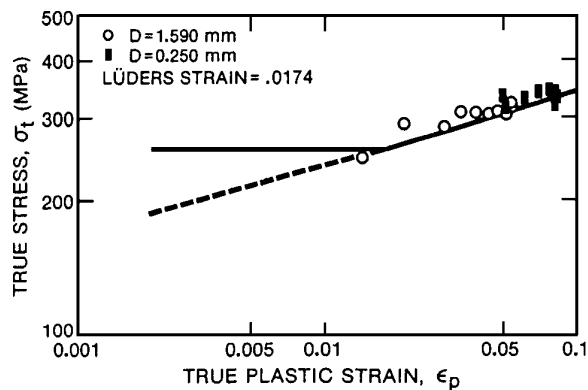


Fig. 8 – Comparison of the hardness/microhardness-derived stress-strain data to the uniaxial tensile stress-strain curve for 1015 steel aged 20 min at 121°C (S4).

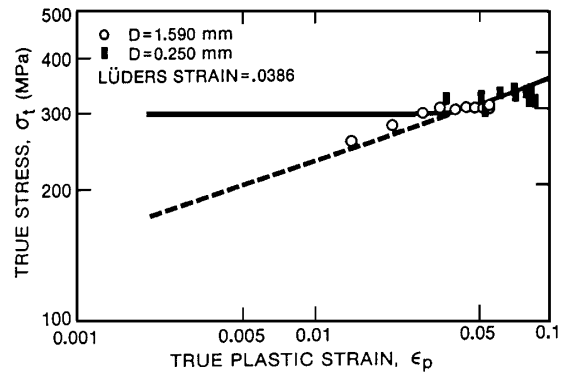


Fig. 9 – Comparison of the hardness/microhardness-derived stress-strain data to the uniaxial tensile stress-strain curve for 1015 steel aged 20 min at 316°C (S11).

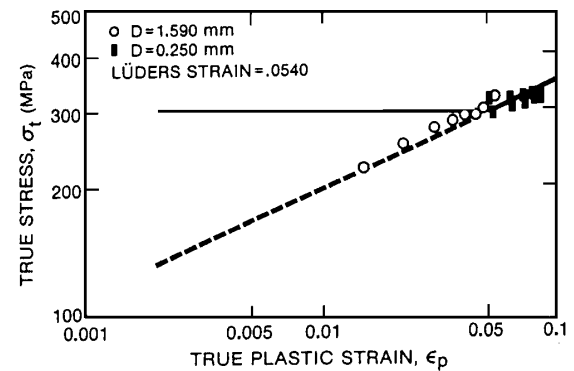


Fig. 10 – Comparison of the hardness/microhardness-derived stress-strain data to the uniaxial tensile stress-strain curve for 1015 steel aged 20 min at 621°C (S20).

V. DISCUSSION

A. Lüders Strain and Indentation Lip Geometry

A definite empirical relationship between the indentation lip geometry and the uniaxial tensile Lüders strain was established both by profilometric and interferometric techniques, and a physically-based explanation can be postulated for such an effect of Lüders strain on indentation geometry. Spherical indentation hardness is a load-controlled test during which the displaced material flows up around the vicinity of the indenter and forms a raised portion surrounding the impression. For work-hardened material the displaced metal forms a raised lip adjacent to the indentation; this effect is known as “piling-up.” On the other hand, with annealed metals, the initial displacement of the metal produces appreciable work-hardening and it becomes easier to displace the adjacent metal; hence, the metal immediately adjacent to the indentation is depressed (a phenomenon called “sinking in”), while the lip is lower in height and spread over a greater region around the indentation.

With this in mind, the material exhibiting high Lüders strain could be considered to behave more like work-hardened material. That is, after yielding in a load-controlled test this material would exhibit a relatively small value of da/de . Hence, a greater

tendency for piling-up of the material occurs. On the other hand, materials exhibiting small Lüders strains would behave more like annealed material. Following yielding in a load controlled test the material would have relatively large values of $d\sigma/d\varepsilon$. Consequently, the material would have a tendency to exhibit less “piling-up” behavior and more “sinking-in” during indentation. Based on this argument, large pile-ups around the indentation would be indicative of large Lüders strains; and this indeed is what has been observed.

It is also important to keep in mind that Lüders strain was not the only flow property which varied in these steels as the heat treatment was varied. As noted earlier, the values of σ_{ly} , K , and n also varied, as they varied in a manner related to ε_L by Morrison's equation:¹⁹

$$\ln \frac{K}{\sigma_{ly}} = \varepsilon_L - n \ln \varepsilon_L \quad [7]$$

Therefore, an empirical correlation between lip geometry and Lüders strain implicitly includes these other flow properties. Again, if an increase in ε_L is also accompanied by an increase in n , as was the case in this study, a greater amount of pile-up would be expected in the material exhibiting large Lüders strain.

B. Characterization of the Indentation Lip Geometry

Although the indentation geometry was characterized by profilometric techniques in most of this work, this approach has the following drawbacks:

1. It was tedious and time consuming.
2. It is extremely difficult to apply to small indentations.
3. This technique provides only a two-dimensional representation of the lip geometry for a single profile trace. This does not permit the asymmetry of the lip to be easily characterized.
4. The diamond stylus of the profilometer scratches the surface of the metal. This could also affect the indentation measurements.

Because of the third and perhaps the fourth drawbacks, a large data scatter existed in the correlation between lip geometry and Lüders strain. Nevertheless, the technique was very helpful in establishing a definite relation between the two.

The interferometry technique, demonstrated briefly in this paper, has the following advantages over the profilometry technique for indentation characterization as an integral part of a microhardness measurement technique:

1. It is relatively easy to apply.
2. The technique is nondestructive; hence, it permits indentation lip characterization periodically in a multiple indentation test. Because of this advantage it should be easier to use this technique on irradiated specimens.
3. Interferometry provides a three-dimensional characterization of the geometry of the indentation lip; whereas profilometry can provide only two-dimensional characterization and hence may result in large uncertainties because of indentation asymmetries.
4. Interferometry may be an important tool to observe other types of inhomogeneous flow, such as dislocation channeling in irradiated materials.
5. It has a high surface topography resolution capability, since the distance between adjacent fringes corresponds to a difference in height of one-half the wave length of the illuminating light.
6. The technique could be incorporated with little foreseeable difficulty as part of a standard ball-modified microhardness tester by attaching an interference objective lens and appropriate light source to the microhardness tester. This will result in a

considerable consolidation of experimental apparatus and a consequent reduction in experimental time and difficulty.

Thus, because of the good agreement between interferometric and profilometric measurements obtained in this work, and the many advantages of the interferometer over the profilometer, application of the interferometric technique is currently being pursued in the follow-on development of microhardness tests for the fusion materials program.

C. Hardness-Tensile Data Correlation

Although good comparison between the hardness/microhardness derived $\sigma_t - \varepsilon_p$ data and the uniaxial tensile $\sigma_t - \varepsilon_p$ curve was obtained, the values of 0.759 and 24, in Eq. [5], obtained by nonlinear regression analysis were somewhat different from those determined by Au³ (0.531 and 27), based on work by Francis.¹⁸ These values of 0.759 and 24, in Eq. [5], result in larger values of ψ for the 1015 steel; for instance, the maximum value of ψ obtained by using these empirical constants is $\psi_{\max} = 3.48$. This value is considerably higher than the value of 2.8 to 3.00 commonly reported^{17, 18, 20, 21} for ψ_{\max} .

This large value of ψ_{\max} (3.48) appears to be the result of a strain rate effect on the flow properties of 1015 steel samples.^{22, 23} Low carbon steels generally have higher strain rate sensitivity values than most other common metals (for this 1015 steel the strain rate sensitivity ranged from 0.05 to 0.07 for the as-received and aged at 621°C specimens, respectively). For material which is strain rate sensitive, then, the maximum value of ψ will be related to the effective strain rates used in hardness and tensile testing ($\dot{\varepsilon}_p$ and $\dot{\varepsilon}_\sigma$, respectively) by²⁴

$$\psi_{\max} = \frac{P_m}{\sigma_{t\max}} \cong 2.8 \left(\frac{\dot{\varepsilon}_p}{\dot{\varepsilon}_\sigma} \right)^m \quad [8]$$

where m is the strain rate sensitivity of the effective flow stress. The value of $\dot{\varepsilon}_\sigma$ for the tensile tests was $6.67 \times 10^{-4} \text{ s}^{-1}$. Mok²² has given an approximate equation for the effective strain associated with a ball indentation test as

$$\dot{\varepsilon}_p = \frac{2}{5} \frac{v}{d} \quad [9]$$

where v is the ball indenter velocity. Since $\dot{\varepsilon}_p$ is a function of d , the value calculated for ψ_{\max} will be different for different indentation sizes. For the hardness and microhardness tests conducted in this study, the calculated values of ψ_{\max} range from 3.04 to 3.86, with an average value of 3.45. This is close to the value of 3.48 obtained from the regression analysis. Hence, although the above derivation is not a rigorous one, it does indicate that the larger values of ψ_{\max} obtained in this study are attributable to strain rate differences between the hardness/microhardness tests and the tensile tests.

VI. CONCLUSIONS

A quantitative correlation between Lüders strain and the geometry of the lip around a ball indentation was found for 1015 steel specimens. The best correlation obtained by both profilometry and optical interferometry is a proportional increase in the volume of material piled up around the indentation as the magnitude of the uniaxial Lüders strain exhibited by the material increases. In addition, a set of equations was developed by which spherical indentation hardness data fit the homogeneous true-stress–true-plastic-strain relation for steels exhibiting a relatively

wide range of constitutive behavior. The combination of hardness/microhardness data and indentation geometry characterization is quite promising for extracting flow property information from small volume specimens.

ACKNOWLEDGEMENTS

The authors would like to thank J. W. Shekherd for his invaluable technical support, and G. R. Odette for many helpful discussions. We would also like to acknowledge the support of the United States Department of Energy, Office of Fusion Energy, for this work.

REFERENCES

¹ G. L. Kulcinski: *Proc. Intl. Conf. On Rad. Eff. And Tritium Tech. For Fusion Reactors*, J. S. Watson and F. W. Wiffen, eds., ORNL, ERDA, ANS, AIME, 1975, vol. I, p. 17.

² *Experimenter's Guide: RTNS-II Facility*, Lawrence Livermore Laboratory, University of California, M-094, July 1978.

³ P. Au, G. E. Lucas, J. W. Shekherd, and G. R. Odette: *Nondestructive Evaluation in the Nuclear Industry*, Metals Park, OH 1981, p. 597.

⁴ G. E. Lucas and N. F. Panayotou: *J. Nucl. Mater.*, 1981, vols. 103 and 104, p. 1527.

⁵ M. Dooley, G. E. Lucas, and J. W. Shekherd: *J. Nucl. Mater.*, 1981, vols. 103 and 104, p. 1533.

⁶ N. F. Panayotou, R. J. Puigh, and E. K. Opperman: *J. Nucl. Mater.*, 1981, vols. 103 and 104, p. 1523.

⁷ E. R. Bradley and R. H. Jones: *J. Nucl. Mater.*, 1981, vols. 103 and 104, p. 901.

⁸ F. H. Huang and G. L. Wire: *J. Nucl. Mater.*, 1981, vols. 103 and 104, p. 1511.

⁹ R. J. Puigh, R. E. Bauer, A. M. Ermi, and B. A. Chin: *J. Nucl. Mater.*, 1981, vols. 103 and 104, p. 1501.

¹⁰ G. L. Wire and F. H. Huang: *Nucl. Tech.*, 1982, vol. 57, p. 234.

¹¹ M. P. Manahan, A. S. Argo, and O. K. Harling: *J. Nucl. Mater.*, 1981, vols. 103 and 104, p. 1545.

¹² G. E. Lucas and C. Pendleton: *J. Nucl. Mater.*, 1981, vols. 103 and 104, p. 1539.

¹³ R. I. Mair and E. E. Banks: *Exp. Mech.*, 1973, vol. 13, p. 77.

¹⁴ V. V. Tan and A. Dubé: *Can. Met. Quart.*, 1971, vol. 10, p. 29.

¹⁵ K. Tanaka and H. Ishikawa: *Proc. Japan. Congr. Mater. Res.*, Society of Materials Science, Kyoto, Japan, 1977, p. 7.

¹⁶ J. H. Underwood: *Exp. Mech.*, 1973, vol. 13, p. 373.

¹⁷ D. Tabor: *The Hardness of Metals*, Clarendon Press, Oxford, 1951, p. 73.

¹⁸ H. A. Francis: *Trans. ASME*, 1976, vol. 98, ser. H, p. 272.

¹⁹ W. B. Morrison: *2nd Int. Conf. On Strength of Metals and Alloys*, ASM, Metals Park, OH 1970, p. 879.

²⁰ C. H. Lee, S. Masaki, and S. Kobayashi: *Int. J. Mech. Sci.*, 1972, vol. 14, p. 417.

²¹ D. J. Abson, O. Kosik, J. L. Uvira, and J. J. Jonas: *The Science of Hardness Testing and Its Research Applications*, J. H. Westbrook and H. Conrad, eds., ASM, Metals Park, OH 1973, p. 91.

²² C. H. Mok: *Exp. Mech.*, 1966, vol. 6, no. 2, p. 87.

²³ J. R. Newby: *Formability Topics – Metallic Materials*, American Society for Testing and Materials, ASTM-STP-647, 1978, p. 4.

²⁴ F. M. Haggag: M.S. Thesis, Department of Chemical and Nuclear Engineering, University of California, Santa Barbara, CA 1980.